Quantified degeneracy, entropy, and metal-insulator transition in complex transition-metal oxides

Jae-Hoon Sim,[1] Siheon Ryee,[1] Hunpyo Lee,[2] and Myung Joon Han[1,3,*]

[1]*Department of Physics, Korea Advanced Institute of Science and Technology (KAIST), Daejeon 34141, Korea*

[2]*Department of General Studies, Kangwon National University, 346 Jungang-ro, Samcheok-si, Kangwon-do 25913, Korea*

[3]*KAIST Institute for the NanoCentury, Korea Advanced Institute of Science and Technology, Daejeon 34141, Korea*

(Received 7 August 2017; revised manuscript received 16 September 2018; published 10 October 2018)

Understanding complex correlated oxides and their phase transitions has long been a challenge. The difficulty largely arises from the intriguing interplay between multiple degrees of freedoms. While degeneracy can play an important role in determining material characteristics, there is no well-defined way to quantify and to unveil its role in real materials having complicated band structures. Here we suggest a way to quantify the "effective degeneracy" relevant to metal-insulator transition by introducing entropylike terms. This new quantity well describes the electronic behaviors of transition-metal oxides as a function of external and internal parameters. With 3*d* titanates, 4*d* ruthenates, and 5*d* iridates as our examples, we show that this new effective quantity provides useful insights to understand these systems and their phase transitions. For $LaTiO_3/LaAlO_3$ superlattice, we suggest a novel "degeneracy control" metal-insulator transition.

DOI: 10.1103/PhysRevB.98.165114

I. INTRODUCTION

Understanding transition-metal oxides (TMOs) and their phase transitions has been a central issue in condensed matter physics and material science. Many of exotic quantum phases of matters are the result of intriguing interplay and competition between the multiple degrees of freedom active in TMOs; namely, charge, spin, orbital, and lattice [1]. Estimating the key parameters which represent those degrees of freedom and their couplings is therefore a crucial step. Quantifying other physical parameters such as bandwidth, crystal field, and interactions (i.e., U, U', and J) is also often posing a nontrivial task. Depending on which parameter is crucial, the metal-insulator transition (MIT) is described and classified into subcategory of "bandwidth control," "filling control," and "dimensionality control" MIT [1].

Orbital degeneracy can certainly play an important role in determining material characteristics of TMOs [2–7]. However, there is no well-defined way to quantify and unveil its role in the coorperation with other physical components of real materials with complicated multiband structures around Fermi energy (E_F). In this study we first try to quantify the "effective" orbital degeneracy by introducing entropylike terms. Then we apply it to real material systems. Our results of 4*d* ruthenates and 5*d* iridates show that this newly introduced quantity well describes the electronic behavior and provides useful insight to understand MIT. Furthermore, we suggest a novel "degeneracy control" MIT in 3*d* titanate superlattice. The strain-dependent phase diagram and the calculated physical parameters clearly show that the transition is governed mainly by "degeneracy" not by other factors such as bandwidth.

Defining an intuitive and computable physical quantity has been playing central roles in quantum material research. "Charge-transfer energy" for TMOs [8] and "Chern number" (or TKNN number) for topological materials [9–11] can be recent examples. Even though both are not directly measurable in experiments, they certainly provide key information to classify and understand a given type of materials. In this regard, the quantified effective degeneracy we suggest here can also be a useful tool to study multiorbital complex oxides and their phase transitions.

II. QUANTIFYING EFFECTIVE DEGENERACY

In model-based studies, the degree of degeneracy is naturally defined by the energy level difference. For real materials, on the other hand, quantifying degeneracy is not always straightforward due to the complicated band structures which is in the end a result of combinations of many other "parameters" such as crystal field levels and hybridizations. Furthermore, we note that the information relevant to MIT is hardly extracted from the "bare" degeneracy represented simply by level differences. With this motivation we define the following quantity:

$$D = \sum_{\mu} S(n_\mu). \tag{1}$$

Here the entropylike term S is given by

$$S(n_\mu) = -n_\mu \log_2 n_\mu - (1 - n_\mu)\log_2(1 - n_\mu), \tag{2}$$

where n_μ is the eigenvalue of on-site number operator $\hat{N}$. The matrix elements of $\hat{N}$ can be written as $N_{\alpha\beta} = \frac{1}{N_{\mathbf{k}}}\sum_{\mathbf{km}}\langle \mathbf{k}m|\alpha\rangle\langle\beta|\mathbf{k}m\rangle$ with orbital indices α and β (i.e., three t_{2g} states in our examples; well represented by Wannier functions), momentum $\mathbf{k}$, and band index m. Note that $N_{\alpha\beta}$ is calculated from the "noninteracting" Hamiltonian, namely, $U = 0$ paramagnetic band structure, which is the same case with other model parameters to be used to understand MIT such as bandwidth (W) and correlation strength (U) [12,13].

*mj.han@kaist.ac.kr

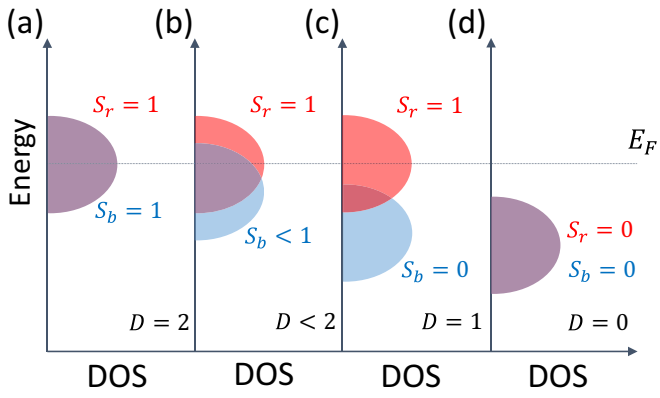

FIG. 1. The behavior of D for some schematic two-orbital electronic structures. In the case of (a), two DOS are fully degenerated and D is maximized, $D = 2$. As two DOS are separated from each other, D is reduced as shown in (b) and (c). As an effective degeneracy (not mere degeneracy) D is being reduced when the on-site orbital energy moves far away from E_F. As shown in (d), even if two DOS are fully degenerated in the usual sense, the calculated $D = 0$ because both states are fully occupied.

While the calculation of D at finite U is straightforward, the useful information is mainly contained in D at $U = 0$.

The eigenstate $|\mu\rangle$ of the on-site number operator does not need to be any of conventional symmetry states ($|\alpha\rangle$), and can be expressed as the superposition of them [14]. S is maximized ($S = 1$) at half-filling ($n_\mu = 0.5$) and minimized ($S = 0$) when the orbital is fully occupied ($n_\mu = 1$) or unoccupied ($n_\mu = 0$). D reflects the number of orbital states at E_F and thus carries similar information with degeneracy. At the same time, D is clearly different from "mere" degeneracy. The number of states is weighted by taking the band position into account with respect to E_F. As a result, D magnifies the information relevant to MIT. In this sense, D can be called as "effective degeneracy." On the other hand, as obvious from Eq. (2), D measures a certain type of entropy being regarded as "effective entropy." For more discussion of its physical meaning, see the Supplemental Material [14].

In order to see how this new quantity works, let us consider a schematic situation presented in Fig. 1. Physically, degeneracy should be largest when the two bands (assumed to have same bandwidths and shapes) are located at the same energy; see Fig. 1(a). It is gradually lifted as two levels become differentiated. Suppose that the band structure evolves from Fig. 1(a) to 1(b) and 1(c) by any parameter change. S_b (corresponding to one of the two bands; blue colored) is gradually reduced from $S_b = 1$ [Fig. 1(a)] to $S_b = 0$ [Fig. 1(c)] while another band (red colored) does not move and S_r is unchanged. When the two density of states (DOS) are identically overlapped with each other [Fig. 1(a)], D is maximized, $D = 2$. When the DOS overlap is minimized [Fig. 1(c)], D is minimized, $D = 1$. Therefore D carries the similar information with degeneracy in the usual sense. At the same time, however, D is different from mere degeneracy as clearly shown in Fig. 1(d). The calculated D of Fig. 1(d) is zero even though two DOS are fully overlapped. This feature demonstrates that D is defined to represent the effective degeneracy or effective entropy of the bands near E_F relevant to MIT. In fact, both DOS in Fig. 1(d) are not relevant to MIT since they are fully occupied and far away from E_F.

D works for more general cases. Consider M orbitals whose on-site energies are given by ε's near E_F [i.e, $|\varepsilon - E_F| \ll W$ (bandwidth)]. For two states per orbital (occupied and unoccupied), the number of configurations is given by $\Omega \sim 2^M$ and $M \sim \log_2 \Omega$. In the case of single electron per site, $D(M) = M \log_2 M - (M-1)\log_2(M-1)$ from $n_\alpha = 1/M$. While $D(M)$ is not equal to but less than M (e.g., $D \sim 3.90$ for $M = 6$), it provides an acceptable measure of degeneracy or entropy for this given model in a general sense.

III. APPLICATIONS TO REAL MATERIALS

The usefulness of this new quantity can be more clearly seen with real examples. Below we take three different systems of $3d$, $4d$, and $5d$ TMOs in which the degeneracy is changed by the internal as well as external parameters. Also, our example sets include both strongly (titanate and iridate; Mott insulators) and moderately correlated (ruthenate in bulk; metals) electron systems. Below, while we define the standard deviation (σ) of Gaussian fitted DOS as the bandwidth, we confirm that the use of Wannier function or Lorentzian fitting does not change any of our conclusions.

A. Ruthenates

In this subsection we apply our effective degeneracy or effective entropy to ruthenate thin films. Recently $SrRuO_3$ (SRO-113) has attracted significant research attention due to its intriguing phase transitions observed as the film thickness is reduced [15–19]. While bulk SRO-113 is a ferromagnetic (FM) metal, its thin film phase is known to become insulating [15–18] and presumably antiferromagnetic (AFM) [16,20,21]. Critical thickness and the concomitance of MIT and magnetic transition still remain unclear [15–19].

Figures 2(a) and 2(b) shows the projected DOS for one-layer ($n = 1$) and three-layer ($n = 3$) film, respectively. As expected, the Ru-t_{2g} states are more degenerate in $n = 3$ being closer to a three-dimensional cubic bulk situation in which the three are completely degenerate. On the other hand, in $n = 1$, d_{xy} state is noticeably different from $d_{yz,zx}$.

Here we first note that this electronic structure change is well described by D in a quantitative manner. As shown in Fig. 2(c), the calculated D is gradually increased as n increases being consistent with the intuition and the band structure result. It shows that the newly defined quantity D works reasonably well for describing the realistic band structure change. Furthermore, our result has a meaningful implication regarding the origin of observed MIT as a function of thickness; not only bandwidth (and/or dimensionality) [19,21] but also degeneracy plays the role in this transition.

The usefulness of D is further demonstrated in the strain-dependent transition. Figures 2(d) and 2(e) presents projected DOS for 2% compressive and tensile strained monolayer thin film, respectively. We note that in this case the degree of degeneracy is not clearly seen without calculating D. The calculated D as a function of strain is presented in Fig. 2(f) showing that D is gradually decreased as more tensile strain is applied. In this sense the DOS of Fig. 2(d) is more degenerate

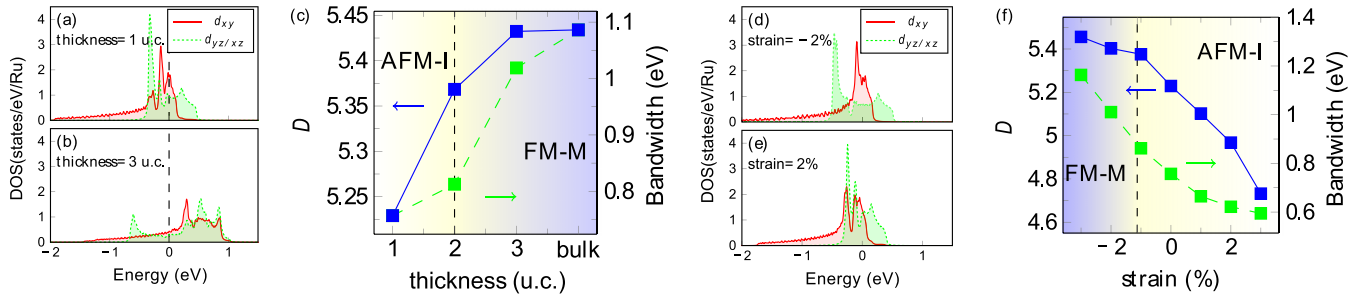

FIG. 2. (a) and (b) The calculated DOS projected onto Ru-t_{2g} states for (a) $n = 1$ and (b) $n = 3$ with zero strain. The vertical dashed lines refer to E_F. (c) The calculated D (blue; left side) and bandwidth (green dashed line; right side) as a function of film thickness n. A transition from FM metal (FM-M; blue) to AFM insulator (AFM-I; yellow) occurs at the thickness of $n = 2$–4. (d) and (e) The calculated DOS projected onto Ru-t_{2g} states for 1-unitcell-thick SRO-113 film with (d) −2% compressive and (e) +2% tensile strain. (f) The calculated D and bandwidth as a function of strain. At around −1% compressive strain, there is a phase transition from FM-M (blue) to AFM-I (yellow). The DOS, D, and bandwidth are calculated from nonspin-polarized ($U = 0$) results while the phase diagrams are constructed from spin-polarized GGA calculations.

than that of Fig. 2(e). This example demonstrates that, even when the intuitive conclusion is not likely reached, D extracts the desired information.

Our result shows that D is not mere degeneracy in the usual sense but reflects the other factors relevant to MIT. According to Eq. (1) the states near E_F contribute more to D than the other states away from E_F. Importantly, the decreasing trend of D as a function of strain is consistent with the decreasing metallicity. It is known that the system becomes more insulating in the tensile strain regime and more metallic in the compressive strain [21]. In this regard, D represents an effective degeneracy or entropy carrying the quantitative information physically relevant to MIT. In the case of DOS in Fig. 2(d), the prominent d_{xy} peak developed around E_F is responsible for larger D (see the Supplemental Material [14]).

B. Iridates

The second example is Sr_2IrO_4 (SIO-214) in which the degeneracy is lifted not by external parameters such as strain and thickness but by spin-orbit coupling (SOC). SIO-214 is known as a "relativistic Mott" insulator in the sense that SOC plays the key role to induce Mott gap [22,23]. Due to the large crystal field and SOC, Ir-t_{2g} states split into so-called $j_{\text{eff}} = 3/2$ quartet and $j_{\text{eff}} = 1/2$ doublet. Whereas different pictures have been discussed [24–30], still quite prevailing is that the main role of SOC is to reduce the bandwidth making relatively small U be enough to open the gap [23,31,32].

Here we show that the calculation of D supplements the understanding of Mott gap formation. Let us first note that SOC cannot only reduce the bandwidth but also lift the degeneracy. This possibility has been speculated in the context of reminiscing about multiorbital Hubbard model studies [28–30]. However, it could not be discussed quantitatively and therefore not examined systematically in comparison to other possibilities [24–27]. Furthermore, a significant amount of hybridization between $j_{\text{eff}} = 1/2$ and $3/2$ has been noted in the literature [28,32,33], which render the simple model analysis more difficult.

Figures 3(a) and 3(b) shows the projected DOS with and without SOC, respectively, and the calculated bandwidth is presented in Fig. 3(c) as a function of SOC strength (λ). In the range of $0 \leqslant \lambda \leqslant 0.5$ eV, the bandwidth is not significantly reduced. Rather, our estimation shows a slight enhancement of bandwidth at the realistic $\lambda = 0.479$ eV. In fact, the bandwidth reduction by SOC is not quite clearly seen in the calculated DOS itself. Figures 3(a) and 3(b) show that the bandwidth of $j_{\text{eff}} = 1/2$ ($\lambda = 0.479$ eV) can be regarded as being comparable with that of t_{2g} ($\lambda = 0$ eV). Thus, it is difficult to conclude that the gap of SIO-214 is attributed to the bandwidth reduction by SOC.

Our new quantity provides useful insight on this issue. The calculated D is presented in Fig. 3(c) whose decreasing trend clearly shows that the effective degeneracy is gradually lifted by SOC. Together with the estimated critical U_c, which follows the same decreasing trend with D [Fig. 3(d)], our results indicate that lifting degeneracy is the main effect of SOC for the gap formation; SIO-214 may still be regarded as a relativistic Mott insulator, but the major role of SOC is not to reduce bandwidth but to lift degeneracy.

C. Titanates and degeneracy control MIT

The final example is a superlattice made of a classical Mott insulator. The material property of $LaTiO_3/LaAlO_3$

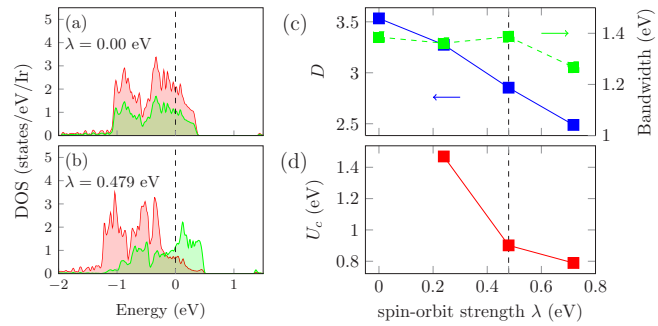

FIG. 3. (a) and (b) The calculated DOS projected onto so-called j_{eff} states (a) without and (b) with SOC. The red and green colored states represent $j_{\text{eff}} = 3/2$ and $1/2$, respectively. The vertical dashed lines correspond to E_F. (c) The calculated bandwidth (green dashed line; right side) of $j_{\text{eff}} = 1/2$ states and D (blue; left side) as a function of λ. Bandwidth are estimated from Gaussian fitting. The realistic value of $\lambda = 0.479$ eV is denoted by the vertical dashed lines. (d) The calculated critical U_c value as a function of λ.

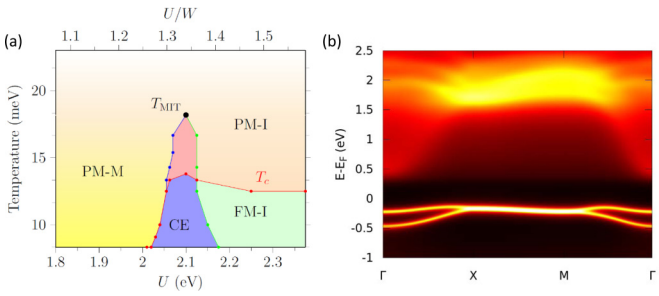

FIG. 4. (a) The U-T phase diagram. The red line indicates the transition from the paramagnetic (PM) to the ferromagnetic (FM) phase. The blue and green lines refer to the transition from metallic-to-insulating, and the insulating-to-metallic state, respectively. CE denotes the coexistence region indicating the first-order transition with an end point at T_{MIT}. (b) The calculated spectral function $A(\mathbf{k}, \omega)$ projected onto Ti with $U = 3$ eV and at $T = 8.3$ meV.

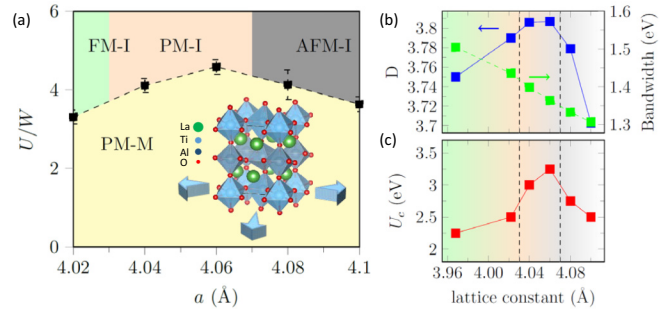

FIG. 5. (a) Strain-dependent DMFT phase diagram in which the dashed line indicates the metal-insulator phase boundary. The metallic region (yellow) is enhanced at $a = 4.06$ Å which corresponds to the degeneracy maximum point. (Inset) Schematic figure for the "strain engineering" of LTO/LAO superlattice. (b) The calculated D (blue; left side) and bandwidth (green dashed line; right side) as a function of in-plane lattice constant. As the more tensile strain applied the bandwidth is gradually decreased as expected. On the other hand, the D is first increased and then decreased with a maximum value at $a = 4.06$ Å. (c) The critical value of U_c as a function of in-plane lattice parameter shows the same trend with D, suggesting that this phase transition is governed mainly by degeneracy.

(LTO/LAO) is an important issue by itself since previous studies show that the electronic and magnetic property are notably different from bulk LTO due to confinement effect [34]. Previous DFT + U calculations show that FM spin and antiferro-orbital order is stabilized [35]. However, no further study has been reported especially using the more advanced techniques beyond static DFT + U, and a part of experimental observations is still not clearly understood [34]. Our DMFT (dynamical mean-field theory) phase diagram is presented in Fig. 4(a). Paramagnetic insulating (PM-I) phase is clearly identified at high temperature and large U regime, which cannot be addressed by static approximations. The calculated spectral function $A(\mathbf{k}, \omega)$ is presented in Fig. 4(b). Coherent features is noticed below E_F [36] and the correct insulating nature is observed with Γ-point gap of 0.48 eV. This gap size is larger than the bulk LTO optical gap (∼0.2 eV) being consistent with the conductivity data on $(\mathrm{LTO})_{1,2,3}/(\mathrm{LAO})_5$ which reports that the lowest energy excitation is gradually moving toward the higher frequency as the LTO layer thickness is reduced [34]. At a realistic value of $U = 3$ eV for the superlattice [35,37], the magnetic transition between ferromagnetic (FM-I) and PM-I occurs at $T_c \simeq 12.5$ meV in good agreement with the total energy difference by GGA + U [35]. Overall, our DMFT results in large-U and low-T limit are consistent with static DFT + U calculations.

Now we consider the strain dependence and "degeneracy control" MIT. Figure 5(a) presents the phase diagram as a function of in-plane lattice parameter. Note that metallic region (yellow) is enlarged at around $a = 4.06$ Å. The calculated D is presented in Fig. 5(b) showing that the effective degeneracy is also maximized at this point. The critical value of U_c [Fig. 5(c)] exhibits the same trend. Our results altogether indicate that the metallicity is enhanced due to orbital fluctuations in the vicinity to the degeneracy maximum point (for more details, see the Supplemental Material [14]).

Importantly, this fluctuation overcomes the effect of reduced bandwidth, thereby triggering the phase transition. The bandwidth is monotonically decreased, see Fig. 5(b), clearly indicating that the competition between metallic and insulating phase is primarily governed by degeneracy. In the current case, so-called "strain engineering" does not just control the bandwidth, but simultaneously change D, and importantly, the governing parameter is (effective) degeneracy. Obviously, the other possibilities such as "dimensionality" and "filling" control MIT are not relevant here.

As often being the case, this MIT is accompanied by magnetic transition at low temperature. As shown in Fig. 5(a), different magnetic phases are stabilized as a function of in-plane lattice constant. While the two end members of this phase diagram (i.e., FM-I and AFM-I) have been reported previously by GGA + U calculation [35], the PM-I phase at the degeneracy maximum point is first identified in the current DMFT study.

IV. SUMMARY

We introduced a new quantity which estimates effective degeneracy relevant to MIT. This quantity denoted by D can be easily calculated and is generally applicable to any real multiorbital systems for which quantifying the degree of degeneracy is often hampered by the complicated band structures. By applying D to $3d$, $4d$, and $5d$ TMO, we show that this newly introduced quantity works well to describe the electronic behavior as a function of external and internal parameters. In particular, we show that the effective degeneracy plays together with bandwidth change in the thickness-dependent transition of SRO-113 and that the "relativistic" effect by SOC in the SIO-214 gap formation is primarily to lift degeneracy rather than to reduce bandwidth. From the strain dependent phase diagram of LTO/LAO superlattice, we suggest a novel "degeneracy control" MIT. While effective degeneracy is not the only component to describe MIT, our examples clearly show that this new quantity provides useful information which cannot be captured by other conventional quantities such as bandwidth and filling.

ACKNOWLEDGMENTS

We thank A. T. Lee, H.-S. Kim, and S. W. Jang for technical helps. J.-H.S., S.R., and M.J.H. were supported by Basic Science Research Program through the National Research Foundation of Korea (NRF) funded by the Ministry of Education (2018R1A2B2005204). The computing resource is supported by National Institute of Supercomputing and Networking/Korea Institute of Science and Technology Information with supercomputing resources (KSC-2015-C3-042).

[1] M. Imada, A. Fujimori, and Y. Tokura, Rev. Mod. Phys. **70**, 1039 (1998).

[2] E. Pavarini, S. Biermann, A. Poteryaev, A. I. Lichtenstein, A. Georges, and O. K. Andersen, Phys. Rev. Lett. **92**, 176403 (2004).

[3] Z. Zhong, M. Wallerberger, J. M. Tomczak, C. Taranto, N. Parragh, A. Toschi, G. Sangiovanni, and K. Held, Phys. Rev. Lett. **114**, 246401 (2015).

[4] A. Georges, L. de' Medici, and J. Mravlje, Annu. Rev. Condens. Matter **4**, 137 (2013).

[5] M. A. Hossain, B. Bohnenbuck, Y. D. Chuang, M. W. Haverkort, I. S. Elfimov, A. Tanaka, A. G. Cruz Gonzalez, Z. Hu, H.-J. Lin, C. T. Chen, R. Mathieu, Y. Tokura, Y. Yoshida, L. H. Tjeng, Z. Hussain, B. Keimer, G. A. Sawatzky, and A. Damascelli, Phys. Rev. B **86**, 041102(R) (2012).

[6] T. F. Qi, O. B. Korneta, S. Parkin, L. E. De Long, P. Schlottmann, and G. Cao, Phys. Rev. Lett. **105**, 177203 (2010).

[7] W. Brzezicki, A. M. Oleś, and M. Cuoco, Phys. Rev. X **5**, 011037 (2015).

[8] J. Zaanen, G. A. Sawatzky, and J. W. Allen, Phys. Rev. Lett. **55**, 418 (1985).

[9] D. J. Thouless, M. Kohmoto, M. P. Nightingale, and M. den Nijs, Phys. Rev. Lett. **49**, 405 (1982).

[10] M. Z. Hasan and C. L. Kane, Rev. Mod. Phys. **82**, 3045 (2010).

[11] X.-L. Qi and S.-C. Zhang, Rev. Mod. Phys. **83**, 1057 (2011).

[12] F. Aryasetiawan, M. Imada, A. Georges, G. Kotliar, S. Biermann, and A. I. Lichtenstein, Phys. Rev. B **70**, 195104 (2004).

[13] S. W. Jang, H. Sakakibara, H. Kino, T. Kotani, K. Kuroki, and M. J. Han, Sci. Rep. **6**, 33397 (2016).

[14] See Supplemental Material at http://link.aps.org/supplemental/10.1103/PhysRevB.98.165114 for details on computational methods and the physical meaning of D, which includes Refs. [2,21,35,38–54].

[15] D. Toyota, I. Ohkubo, H. Kumigashira, M. Oshima, T. Ohnishi, M. Lippmaa, M. Takizawa, A. Fujimori, K. Ono, M. Kawasaki, and H. Koinuma, Appl. Phys. Lett. **87**, 162508 (2005).

[16] J. Xia, W. Siemons, G. Koster, M. R. Beasley, and A. Kapitulnik, Phys. Rev. B **79**, 140407(R) (2009).

[17] G. Koster, L. Klein, W. Siemons, G. Rijnders, J. S. Dodge, C.-B. Eom, D. H. A. Blank, and M. R. Beasley, Rev. Mod. Phys. **84**, 253 (2012).

[18] K. Ishigami, K. Yoshimatsu, D. Toyota, M. Takizawa, T. Yoshida, G. Shibata, T. Harano, Y. Takahashi, T. Kadono, V. K. Verma, V. R. Singh, Y. Takeda, T. Okane, Y. Saitoh, H. Yamagami, T. Koide, M. Oshima, H. Kumigashira, and A. Fujimori, Phys. Rev. B **92**, 064402 (2015).

[19] Y. J. Chang, C. H. Kim, S.-H. Phark, Y. S. Kim, J. Yu, and T. W. Noh, Phys. Rev. Lett. **103**, 057201 (2009).

[20] L. Si, Z. Zhong, J. M. Tomczak, and K. Held, Phys. Rev. B **92**, 041108(R) (2015).

[21] S. Ryee and M. J. Han, Sci. Rep. **7**, 4635 (2017).

[22] B. J. Kim, H. Ohsumi, T. Komesu, S. Sakai, T. Morita, H. Takagi, and T. Arima, Science **323**, 1329 (2009).

[23] B. J. Kim, H. Jin, S. J. Moon, J.-Y. Kim, B.-G. Park, C. S. Leem, J. Yu, T. W. Noh, C. Kim, S.-J. Oh, J.-H. Park, V. Durairaj, G. Cao, and E. Rotenberg, Phys. Rev. Lett. **101**, 076402 (2008).

[24] R. Arita, J. Kuneš, A. V. Kozhevnikov, A. G. Eguiluz, and M. Imada, Phys. Rev. Lett. **108**, 086403 (2012).

[25] A. Yamasaki, S. Tachibana, H. Fujiwara, A. Higashiya, A. Irizawa, O. Kirilmaz, F. Pfaff, P. Scheiderer, J. Gabel, M. Sing, T. Muro, M. Yabashi, K. Tamasaku, H. Sato, H. Namatame, M. Taniguchi, A. Hloskovskyy, H. Yoshida, H. Okabe, M. Isobe, J. Akimitsu, W. Drube, R. Claessen, T. Ishikawa, S. Imada, A. Sekiyama, and S. Suga, Phys. Rev. B **89**, 121111(R) (2014).

[26] H. Zhang, K. Haule, and D. Vanderbilt, Phys. Rev. Lett. **111**, 246402 (2013).

[27] D. Hsieh, F. Mahmood, D. H. Torchinsky, G. Cao, and N. Gedik, Phys. Rev. B **86**, 035128 (2012).

[28] C. Martins, M. Aichhorn, L. Vaugier, and S. Biermann, Phys. Rev. Lett. **107**, 266404 (2011).

[29] T. Sato, T. Shirakawa, and S. Yunoki, Phys. Rev. B **91**, 125122 (2015).

[30] A. Georges, S. Florens, and T. Costi, J. Phys. IV (France) **114**, 165 (2004).

[31] K. Ishii, I. Jarrige, M. Yoshida, K. Ikeuchi, J. Mizuki, K. Ohashi, T. Takayama, J. Matsuno, and H. Takagi, Phys. Rev. B **83**, 115121 (2011).

[32] H. Watanabe, T. Shirakawa, and S. Yunoki, Phys. Rev. Lett. **105**, 216410 (2010).

[33] S. Mohapatra, J. van den Brink, and A. Singh, Phys. Rev. B **95**, 094435 (2017).

[34] S. S. A. Seo, M. J. Han, G. W. J. Hassink, W. S. Choi, S. J. Moon, J. S. Kim, T. Susaki, Y. S. Lee, J. Yu, C. Bernhard, H. Y. Hwang, G. Rijnders, D. H. A. Blank, B. Keimer, and T. W. Noh, Phys. Rev. Lett. **104**, 036401 (2010).

[35] A. T. Lee and M. J. Han, Phys. Rev. B **89**, 115108 (2014).

[36] M. Daghofer, K. Wohlfeld, A. M. Oleś, E. Arrigoni, and P. Horsch, Phys. Rev. Lett. **100**, 066403 (2008).

[37] Y. Weng and S. Dong, J. Appl. Phys. **117**, 17C716 (2015).

[38] J. P. Perdew, K. Burke, and M. Ernzerhof, Phys. Rev. Lett. **77**, 3865 (1996).

[39] G. Kresse and D. Joubert, Phys. Rev. B **59**, 1758 (1999).

[40] M. J. Han, T. Ozaki, and J. Yu, Phys. Rev. B **73**, 045110 (2006).

[41] http://www.openmx-square.org.

[42] T. Ozaki and H. Kino, Phys. Rev. B **69**, 195113 (2004).

[43] T. Ozaki, Phys. Rev. B **67**, 155108 (2003).

[44] S. L. Dudarev, G. A. Botton, S. Y. Savrasov, C. J. Humphreys, and A. P. Sutton, Phys. Rev. B **57**, 1505 (1998).

[45] N. Mazari and D. Vanderbilt, Phys. Rev. B **56**, 12847 (1997).
[46] I. Souza, N. Mazari, and D. Vanderbilt, Phys. Rev. B **65**, 035109 (2001).
[47] F. Alet, P. Dayal, A. Grzesik, A. Honecker, M. Körner, A. Läuchli, S. R. Manmana, I. P. McCulloch, F. Michel, R. M. Noack, G. Schmid, U. Schollwöck, F. Stöckli, S. Todo, S. Trebst, M. Troyer, P. Werner, and S. Wessel, J. Phys. Soc. Jpn. **74**, 30 (2005).
[48] E. Gull, A. J. Millis, A. I. Lichtenstein, A. N. Rubtsov, M. Troyer, and P. Werner, Rev. Mod. Phys. **83**, 349 (2011).
[49] E. Gull, P. Werner, S. Fuchs, B. Surer, T. Pruschke, and M. Troyer, Comput. Phys. Commun. **182**, 1078 (2011).
[50] M. Jarrell and J. E. Gubernatis, Phys. Rep. **269**, 133 (1996).
[51] O. Gunnarsson, M. W. Haverkort, and G. Sangiovanni, Phys. Rev. B **81**, 155107 (2010).
[52] S. Florens, A. Georges, G. Kotliar, and O. Parcollet, Phys. Rev. B **66**, 205102 (2002).
[53] O. Gunnarsson, E. Koch, and R. M. Martin, Phys. Rev. B **54**, R11026 (1996).
[54] M. A. Nielsen and I. L. Chuang, *Quantum Computation and Quantum Information* (Cambridge University Press, Cambridge, 2010).